Nonreceptor tyrosine phosphatase Shp2 promotes adipogenesis through inhibition of p38 MAP kinase

Zhao He[a], Helen H. Zhu[a], Timothy J. Bauler[b], Jing Wang[a], Theodore Ciaraldi[c], Nazilla Alderson[a], Shuangwei Li[a], Marie-Astrid Raquil[a], Kaihong Ji[a], Shufen Wang[a], Jianhua Shao[d], Robert R. Henry[c], Philip D. King[b], and Gen-Sheng Feng[a,1]

[a]Department of Pathology and Division of Biological Sciences, University of California at San Diego, La Jolla, CA 92093-0864; [b]Department of Microbiology and Immunology, University of Michigan, Ann Arbor, MI 48109-5620; and [c]Veteran's Administration San Diego Healthcare System and Department of Medicine, and [d]Department of Pediatrics, University of California at San Diego, La Jolla,CA 92093

Edited by Marc Montminy, The Salk Institute for Biological Studies, La Jolla, CA, and approved November 12, 2012 (received for review July 31, 2012)

The molecular mechanism underlying adipogenesis and the physiological functions of adipose tissue are not fully understood. We describe here a unique mouse model of severe lipodystrophy. Ablation of *Ptpn11/Shp2* in adipocytes, mediated by *aP2-Cre*, led to premature death, lack of white fat, low blood pressure, compensatory erythrocytosis, and hepatic steatosis in $Shp2^{fat-/-}$ mice. Fat transplantation partially rescued the lifespan and blood pressure in $Shp2^{fat-/-}$ mice, and administration of leptin also restored partially the blood pressure of mutant animals with endogenous leptin deficiency. Consistently, homozygous deletion of Shp2 inhibited adipocyte differentiation from embryonic stem (ES) cells. Biochemical analyses suggest a Shp2-TAO2-p38-p300-PPARγ pathway in adipogenesis, in which Shp2 suppresses p38 activation, leading to stabilization of p300 and enhanced PPARγ expression. Inhibition of p38 restored adipocyte differentiation from $Shp2^{-/-}$ ES cells, and p38 signaling is also suppressed in obese patients and obese animals. These results illustrate an essential role of adipose tissue in mammalian survival and physiology and also suggest a common signaling mechanism involved in adipogenesis and obesity development.

transduction | preadipocyte | dephosphorylation | substrate trapping

Obesity is a high-risk factor for type 2 diabetes, hypertension, liver disorders, and some types of cancer (1, 2). Identification of leptin, an adipokine secreted by adipocytes, is evidently a breakthrough in understanding the physiology of energy balance and obesity (3, 4). The urgency of fighting against obesity and its comorbid conditions calls for better understanding of adipogenesis and the physiological functions of adipose tissue. Although the molecular mechanisms are not fully understood, adipocyte fate determination and differentiation are regulated by several pathways (5). Peroxisome proliferator-activated receptor gamma (PPARγ) and CCAAT/enhancer binding proteins (C/EBPs) are master transcription factors involved in adipogenesis and obesity development (6–8). Moreover, p300, a histone acetyltransferase (9), has been shown to promote adipogenesis through regulation of *PPARγ* and *C/EBPβ* expression (10, 11). Despite a wealth of knowledge at the transcription level (5), intracellular signaling cascades underlying adipogenesis are not fully understood, with fragmented or controversial data in the literature (12–14).

Shp2, encoded by *Ptpn11*, is a tyrosine phosphatase possessing two Src-homology 2 (SH2) domains that operates in leptin signaling by docking on phosphorylated Tyr985 in the intracellular domain of leptin receptor LepRb (15). However, the Shp2 function in the leptin pathway was obscured by the fact that p-Tyr985 is also a binding site for Socs3 (suppressor of cytokine signaling 3) (16). Notably, development of obesity and leptin resistance were observed in mice with Shp2 deleted broadly in the brain (17), selectively in forebrain neurons (18), or more specifically in POMC neurons (19). These results indicate a positive role of Shp2 in amplification of leptin signal in the hypothalamic control of body weight and energy balance. Consistently, selective expression of a dominant active mutant of Shp2 in forebrain neurons enhanced leptin sensitivity in rodents (20).

In contrast, we show here that selective deletion of *Ptpn11/Shp2* in adipose tissue inhibits adipogenesis, resulting in severe lipodystrophy and early postnatal lethality in $Shp2^{fat-/-}$ mice. Despite a major public health concern on morbid obesity, our results suggest that the adipose tissue is required for mammalian survival due to its endocrine function.

Results

Shp2 Ablation in Adipocytes Causes Severe Lipodystrophy and Premature Death. To dissect the molecular mechanism underlying adipogenesis, we generated a mutant mouse line with selective deletion in adipose tissue of Shp2, a modulator of multiple pathways (21, 22). $Shp2^{flox/flox}$ (or $Shp2^{fl/fl}$) mice were crossed with *aP2-Cre* transgenic mice (23), to produce a $Shp2^{fl/fl}$:*aP2-Cre*$^{+}$ ($Shp2^{fat-/-}$) line. Immunoblot analysis showed that Shp2 expression was selectively reduced in fat tissue of $Shp2^{fat-/-}$ mice, compared with several other tissues and organs (Fig. 1*A* and Fig. S1). Most mutants displayed significantly smaller body sizes and lower body weights than littermates 1 wk after birth (Fig. 1 *B* and *C*). The indexes of white adipose tissue (WAT) or liver to body weight were significantly decreased in mutants, although no difference was detected for the ratio of brown adipose tissue (BAT) to body weight (Fig. 1*D*). The lean mass was also lower in mutants but the ratio of lean to body weight was not changed (Fig. S2*A*). Thus, $Shp2^{fat-/-}$ mice exhibited a severe lipodystrophic phenotype, with little s.c. or visceral WAT (Fig. 1*E* and Fig. S2*B*). In less affected mutants, tiny fat pads could be observed, but the sizes of adipocytes were much smaller than in WT controls (Fig.1*F*). Immunoblotting showed no change in expression levels of PTP1B (Fig. S2*D*), a PTP known to associate with obesity (24), in $Shp2^{fat-/-}$ mice.

As noted previously, *Cre* expression is restricted to adipocytes in this *aP2-Cre* mouse line, with no expression detectable in macrophages (Fig. S3*A*) (23). However, to clarify this issue, we generated $Shp2^{fl/fl}$:*adiponectin-Cre*$^{+}$ mice (25), to delete Shp2 in adipocytes. As shown in Fig. S3 *B–D*, immunoblot analysis detected only a slight reduction of Shp2 expression in adipocytes and, consistently, no obvious phenotype was observed in $Shp2^{fl/fl}$:*adiponectin-Cre*$^{+}$ mice, similar to results previously reported (26). To explore a possible effect of Shp2 deletion in macrophages on

Author contributions: Z.H. and G.-S.F. designed research; Z.H., H.H.Z., T.J.B., J.W., N.A., S.L., M.-A.R., K.J., and S.W. performed research; T.C., J.S., R.R.H., and P.D.K. contributed new reagents/analytic tools; Z.H., H.H.Z., J.W., and G.-S.F. analyzed data; and Z.H. and G.-S.F. wrote the paper.

The authors declare no conflict of interest.

This article is a PNAS Direct Submission.

[1]To whom correspondence should be addressed. E-mail: gfeng@ucsd.edu.

See Author Summary on page 21 (volume 110, number 1).

This article contains supporting information online at www.pnas.org/lookup/suppl/doi:10.1073/pnas.1213000110/-/DCSupplemental.

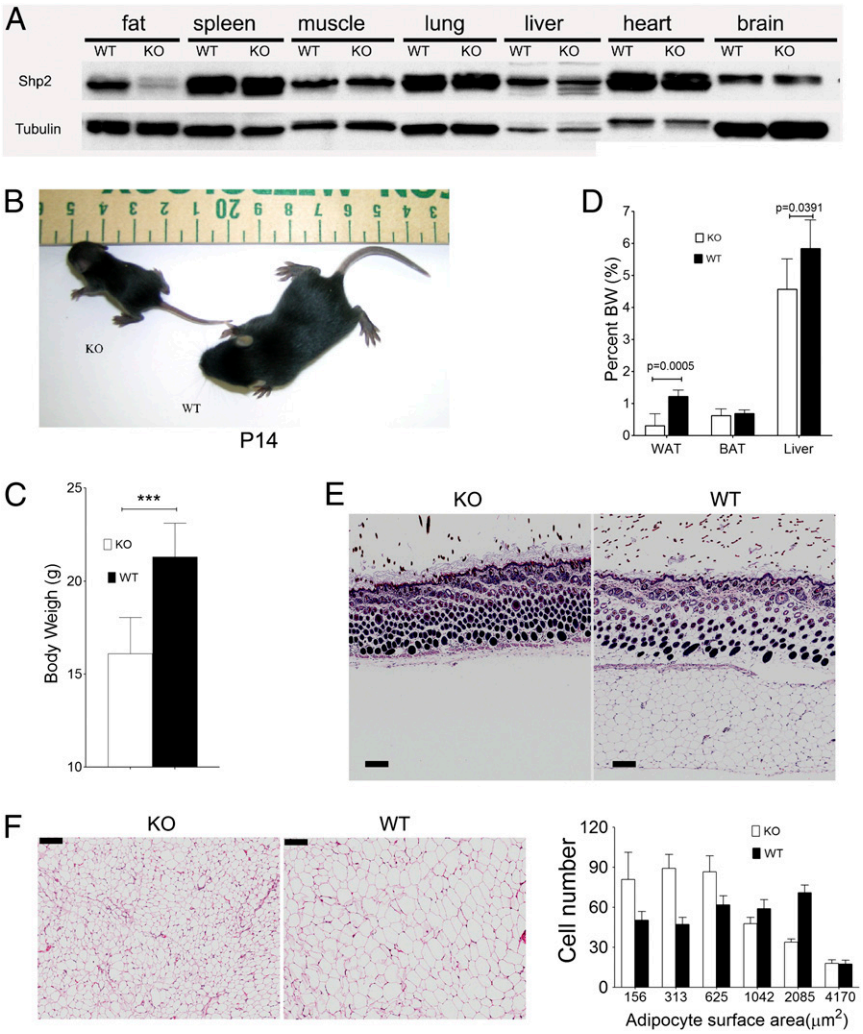

Fig. 1. Shp2 deletion in adipose tissue causes severe lipodystrophy. (*A*) Immunoblotting was performed to determine Shp2 protein amounts in various tissues isolated from control (WT) and *Shp2*$^{fat-/-}$ (KO) mice, as indicated. (*B*) A representative pair of WT and *Shp2*$^{fat-/-}$ littermates at postnatal day 14, showing smaller body size of KO than of WT control. (*C*) The body weights were compared between WT and KO littermates of the same sex at the same ages (n = 11, 4–5 wk old). (*D*) WT and KO mice were compared for their indexes of white adipose tissue (WAT), brown adipose tissue (BAT), or liver vs. body weight (n = 9). (*E*) H&E staining of skin sections shows lack of s.c. fat tissue in *Shp2*$^{fat-/-}$ mice. (Scale bar: 100 μm.) (*F*) White adipocyte sizes from gonadal fat were compared between WT and KO mice. (*Left*) H&E staining. (Scale bar: 100 μm.) (*Right*) Statistical analysis (n = 4).

the lipodystrophy phenotype, we also generated *Shp2*$^{flox/flox}$*:LysM-Cre* mice, which allows for ablation of Shp2 in monocytes/macrophages (27). Immunoblotting showed that Shp2 expression was significantly reduced in macrophages of *Shp2*$^{fl/fl}$*:LysM-Cre*$^{+}$ mice. However, the mutant mice were healthy and indistinguishable from WT controls, excluding the possibility that loss of Shp2 in macrophages played a major role in lipodystrophy in *Shp2*$^{fat-/-}$ mice (Fig. S3 *E* and *F*).

Strikingly, all *Shp2*$^{fat-/-}$ mice died within 3 mo (Fig. 2*A*). The most severely affected ones died before postnatal day 30, with no fat tissue at all, the median group died in 35–55 d and exhibited mildly reduced body weight and sizes, and the less affected mutants that died after 60 d were similar to WT littermates in body weight and sizes. The longevity correlated well with body weights and phenotype severity (Fig. S4), and mice at age of 1 mo or older were used for further analyses.

To determine directly whether the premature death is due to lipodystrophy, we performed adipose tissue transplantation. Gonadal and s.c. fat pads were isolated from WT littermates and were implanted s.c. into *Shp2*$^{fat-/-}$ mutants. As shown in Fig. 2*B*, the sham group of mice died before 90 d, but the fat pad recipients showed prolonged lifespan up to 130 d, indicating that fat transplantation partially rescued the early postnatal death phenotype of *Shp2*$^{fat-/-}$ mice. This observation indicates that the lipodystrophy phenotype is an adipose-autonomous effect of Shp2 removal and that the adipose tissue is required for survival of mammals.

***Shp2*$^{fat-/-}$ Mice Are Defective in Production of Adipokines.** To probe the mechanism underlying premature death associated with lipodystrophy, we measured serum levels of adipokines and growth factors in *Shp2*$^{fat-/-}$ mice, WT controls, and fat-transplanted *Shp2*$^{fat-/-}$ recipients. Levels of leptin, adiponectin, and resistin were significantly lower in *Shp2*$^{fat-/-}$ mice than in controls (Fig. 3 *A*–*C*), whereas the concentrations of PAI-1, IGF1, TNF-α, and MCP-1 were similar between mutant and WT mice (Fig. S5 *A*–*D*). Remarkably, serum levels of leptin and adiponectin were restored to WT levels in *Shp2*$^{fat-/-}$ mice that received fat transplantation (Fig. 3 *A* and *B*), although resistin levels in transplanted mice were similar to those in Shp2 $^{fat-/-}$ mice (Fig. 3*C*). *Shp2*$^{fat-/-}$ mice were too sick to survive the glucose or insulin tolerance test. Serum levels of both insulin and glucose were significantly re-

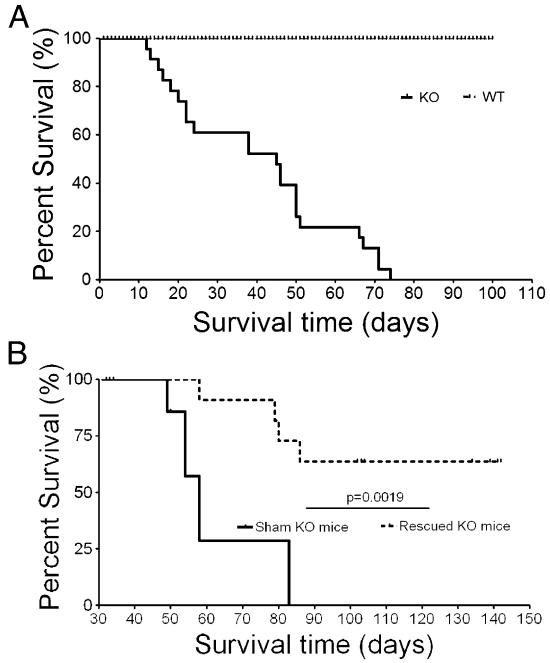

Fig. 2. *Shp2*$^{fat-/-}$ mice die of severe lipodystrophy at early postnatal stage. (*A*) The survival curve for WT and KO mice (n = 23). (*B*) Fat transplantation was performed on *Shp2*$^{fat-/-}$ mice at age 1 mo or older. The lifespan of fat recipients was compared with that of the sham group (sham, n = 8; KO rescued, n = 16).

duced in *Shp2*$^{fat-/-}$ mice, compared with WT controls, and fat transplantation rescued the two important metabolic parameters to WT levels (Fig. 3 *D* and *E*).

Fatty acids are mainly synthesized in the liver and transported into adipose tissue for storage. The lipodystrophic phenotype of *Shp2*$^{fat-/-}$ mice prompted us to investigate hepatic lipid metabolism and the serum concentrations of various types of lipids. As shown in Fig. S5*E*, total serum triglyceride levels in *Shp2*$^{fat-/-}$ mice were higher than in littermate controls, but triglycerides in a mixture of different age mice were similar in mutants, WT, and fat recipients. The amounts of cholesterol, HDL, and LDL/VLDL were also similar between mutants and controls (Fig. 3 *F*–*H*). Consistent with human subjects suffering the lipodystrophy syndrome, *Shp2*$^{fat-/-}$ mice developed severe hepatic steatosis compared with littermate controls (Fig. 3*I*). These data indicate that the deficiency of adipose tissue in *Shp2*$^{fat-/-}$ mice is not due to impaired lipid transportation in circulation but rather a signaling defect intrinsic to adipocytes devoid of Shp2.

Shp2$^{fat-/-}$ Mice Exhibit Low Blood Pressure and Compensatory Erythrocytosis. In identifying the cause of premature death, we observed a splenomegaly phenotype in *Shp2*$^{fat-/-}$ mice (Fig. 4 *A* and *B*), and the ratio of blood cell pellet to serum was dramatically increased in mutants compared to WT mice (Fig. 4*C*). Indeed, the number of red blood cells (RBCs) was remarkably higher in *Shp2*$^{fat-/-}$ mice than in littermate controls (Fig. 4*D*). Hemoglobin (HGB), hematocrit (HCT), mean corpuscular volume (MCV), mean corpuscular hemoglobin (MCH), and red cell distribution width (RCDW), but not mean corpuscular hemoglobin concentration (MCHC), were significantly increased in mutant animals (Fig. 4 *E*–*J*). In particular, the value of HGB that is used to distribute oxygen from erythrocytes to other tissues was dramatically elevated in *Shp2*$^{fat-/-}$ mice, indicating a compensatory response to a status of oxygen shortage (Fig. 4*E*). The number of platelets (PLT), but not platelet hematocrit (PCT) or platelet distribution width (PDW), was decreased in *Shp2*$^{fat-/-}$ mice, compared with WT and fat-transplant recipients (Fig. 4 *K*–*M*). The number of white blood cells was similar between WT and mutant mice (Fig. S6). Fat transplantation rescued the deficient blood phenotype, in particular the RBC and HGB values in *Shp2*$^{fat-/-}$ recipients (Fig. 4 *D* and *E*), identifying lipodystrophy as the cause of blood disorder and oxygen deficit. Further analyses showed that *Shp2*$^{fat-/-}$ mice exhibited lower systolic and diastolic blood pressure accompanied by higher heart beat rate (Fig. 5*A* and Fig. S7*A*). Fat transplantation partially restored the blood pressure, including systolic and diastolic, and heart rates (Fig. 5*A* and Fig. S7*A*). Therefore, the premature death of *Shp2*$^{fat-/-}$ mice is likely due to hypotension, caused by lipodystrophy.

Next, we explored the molecular mechanism underlying low blood pressure in *Shp2*$^{fat-/-}$ mice. In obese patients, leptin levels are positively correlated with blood pressure, and hyperleptinemia is thought to induce hypertension in obese subjects (28–30). As the leptin level was extremely low in *Shp2*$^{fat-/-}$ mice (Fig. 3*A*), we asked whether leptin deficiency is responsible for low blood pressure in the mutants. Real-time monitoring of blood pressure was performed before and after administration of leptin in WT and mutant mice. Following leptin injection, the blood pressure of *Shp2*$^{fat-/-}$ mice, including systolic and diastolic as well as heart rate, was restored to normal levels (Fig. 5*B* and Fig. S7 *B* and *C*). These data suggest that the decreased leptin level caused by lipodystrophy accounts for the low blood pressure in *Shp2*$^{fat-/-}$ mice, supporting a physiological role of leptin in maintaining normal blood pressure in mammals.

Shp2 Mediates PPARγ Expression Through Inhibition of p38 Signaling. Lipodystrophy in *Shp2*$^{fat-/-}$ mice suggests that Shp2 acts to transmit signals required for adipogenesis. To pinpoint the role of Shp2, we collected the tiny residual adipose tissue from the less severe mutant mice, to search for defects in pathways implicated in adipogenesis. Immunoblot analysis showed that the PPARγ protein level, but not that of C/EBPβ, was significantly reduced in Shp2-deficient fat tissue compared with that in controls (Fig. 6*A*), and the mRNA level of PPARγ was also markedly decreased in *Shp2*$^{fat-/-}$ mice (Fig. 6*B*). Previous observations suggest that p300 promotes adipogenesis by binding to the *PPARγ* promoter and enhancing PPARγ expression (10, 31). p300 protein amount was dramatically reduced in Shp2-deficient adipose tissue, with no change in its mRNA level (Fig. 6 *A* and *B*). By examining the mRNA or protein amounts, we did not detect significant changes in the expression of *CREB* and *CEBPβ* in Shp2-deficient fat tissue, with a mild increase in *Pref1* mRNA level (Fig. 6 *A* and *B*). This result suggests that decreased p300 protein content leads to reduced expression of PPARγ. As p38 kinase was shown to promote p300 degradation by phosphorylating p300 (32), we examined the activation status of p38. Notably, the phosphorylation level of p38 was remarkably elevated in Shp2-deficient adipocytes, compared with that in controls (Fig. 6*A*). Together, these data suggest a Shp2-p38-p300-PPARγ signaling event, in which Shp2 promotes adipogenesis through inhibition of p38, thereby promoting p300 stability and PPARγ expression.

We confirmed this signaling mechanism for adipogenesis, using 3T3-L1 preadipocytes in vitro. Knockdown of Shp2 by RNAi resulted in a significant decrease of p300 protein level and PPARγ expression in 3T3-L1 cells (Fig. 6*C*). Following treatment with protease inhibitor MG132 for 1 h, p300 protein level was increased in Shp2 knockdown cells (Fig. 6*D*), suggesting an accelerated degradation of p300 in Shp2-deficient cells. Consistently, p38 phosphorylation was increased in Shp2 knockdown cells (Fig. 6*C*), similar to the phenotype of Shp2 knockout adipocytes (Fig. 6*A*), suggesting an inhibitory effect of Shp2 on p38 activation. Similar to the effect of MG132, treatment with a p38 inhibitor also suppressed p300 protein degradation in Shp2 knockdown cells (Fig. 6*D*).

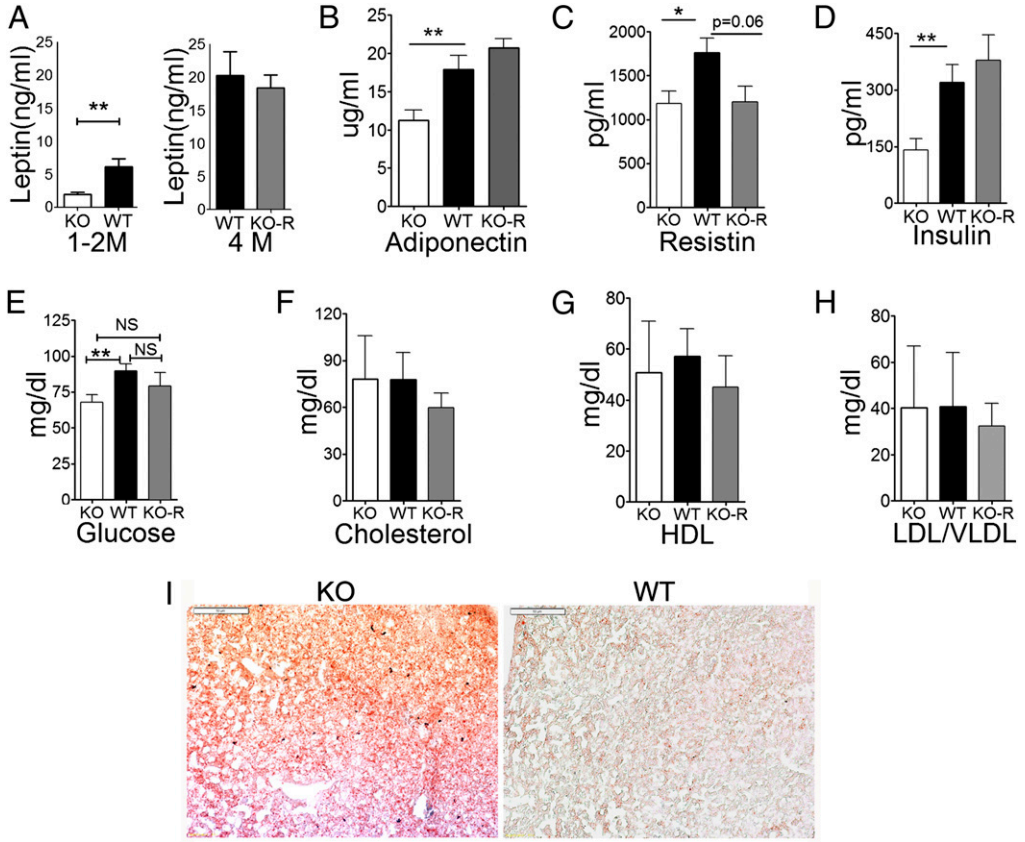

Fig. 3. Ablation of Shp2 in adipose tissue alters adipokine expression. (*A–C*) Serum leptin, adiponectin, and resistin levels were measured in WT (n = 10), KO ($Shp2^{fat-/-}$, n = 10), and KO-R (fat-transplanted $Shp2^{fat-/-}$, n = 6) mice. (*D*) Serum insulin levels were measured in WT, KO, and KO-R mice (WT, n = 11; KO, n = 12; KO-R, n = 6), (*E*) Blood glucose concentrations were compared between WT, KO, and KO-R mice (WT, n = 11; KO, n = 12; KO-R, n = 6). (*F–H*) Total cholesterol, HDL, and LDL/VLDL levels were compared between WT, KO, and KO-R mice (n = 10). (*I*) Liver sections of WT and KO mice were subjected to oil-red staining. (Scale bar: 100 μm.)

We determined the molecular mechanism by which Shp2 modulates p38 MAP kinase activity. Although Shp2 can be coimmunoprecipiated with p38, purified Shp2 enzyme did not dephosphorylate p38 in vitro (Fig. S8*A*), suggesting that Shp2 and p38 coexist in the same complex but p38 is unlikely a direct substrate for Shp2. Acting upstream, a number of kinases, such as TAO, TAK, and DLK that are collectively called MAP KKK, activate MKK3/4/6 (MAP KK), which in turn activates p38 directly (13, 33, 34). As revealed by coimmunoprecipitation, Shp2 was associated with TAO2 and selectively dephosphorylated TAO2 in a phosphatase-dependent manner in vitro (Fig. 6*E* and Fig. S8*B*), indicating that TAO2 is likely a Shp2 substrate. A substrate-trapping assay with vanadate competition verified that Shp2 can interact and dephosphorylate TAO2 (Fig. 6*F*). Consistently, the phosphorylation levels of MKK3/6 and TAO2 were significantly increased in Shp2 knockout or knockdown cells and reexpression of Shp2 restored the inhibition on phosphorylation of MKK3/6 and TAO2 (Fig. 6 *G* and *H*). Together, these data suggest that Shp2 regulates the p38-p300-PPARγ signaling pathway, by controlling the upstream kinase TAO2 activity, in promoting adipogenesis.

Inhibition of p38 Restores Adipocyte Differentiation from $Shp2^{-/-}$ ES Cells. Next, we determined the physiological significance for Shp2 inhibition of p38 signaling in adipogenesis. In $Shp2^{fat-/-}$ mice, Shp2 deletion is controlled by *aP2-Cre*, the expression of which initiates at midgestation (35), suggesting a requirement for Shp2 in the very early stage of prenatal adipogenesis. To address this issue, we resorted to pluripotent embryonic stem (ES) cells that can differentiate into various cell types in vitro. Control and homozygous Shp2 knockout ($Shp2^{-/-}$) ES cell lines were established as previously reported (36). Under regular adipocyte differentiation conditions without dexamethasone, adipocytes were hardly observed in $Shp2^{-/-}$ ES cell culture compared with WT controls, indicating that Shp2 ablation suppresses adipogenesis from ES cells (Fig. 6*I* and Fig. S8*C*). Treatment of p38 inhibitor recovered adipocyte differentiation from $Shp2^{-/-}$ ES cells (Fig. 6*I* and Fig. S8 *D* and *E*). Rosiglitazone (TZD), an agonist of PPARγ, did not restore adipocyte differentiation of $Shp2^{-/-}$ ES cells (Fig. 6*I*). However, combined treatment of p38 inhibitor with TZD rescued adipocyte differentiation of $Shp2^{-/-}$ ES cells (Fig. 6*I*). Taken together, these results indicate a critical role of Shp2 in promoting adipogenesis through increasing PPARγ transcription, which requires inhibition of p38 signaling.

p38 Phosphorylation Is Reduced in Fat or Old Mice and Obese Human Subjects. The results described above suggest a role of Shp2-mediated p38 inhibition in adipogenesis. We then asked whether inhibition of p38 is also involved in development of obesity in adults. To address this point, we evaluated p38 phosphorylation levels in adipose tissue in mice at different ages or in obese mice induced by a high-fat diet (HFD). Indeed, phosphorylation levels of p38 were progressively decreased in an age-dependent manner and also in obese mice fed a HFD, compared with the same age group on chow food (Fig. 7 *A* and *B*). Overall, p38 phosphorylation levels correlated negatively with aging and obesity.

We also assessed p38 phosphorylation levels in lean and obese human subjects with different body mass index (BMI) values.

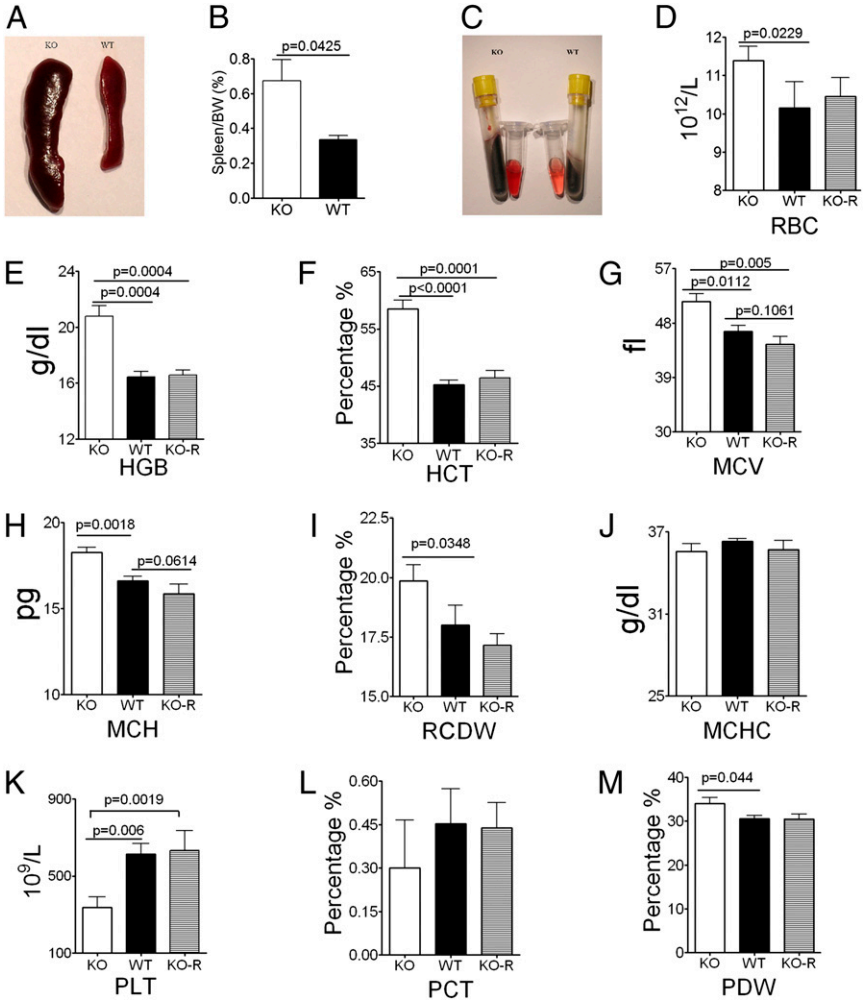

Fig. 4. Shp2$^{fat-/-}$ mice exhibit signs of oxygen shortage (64). A representative spleen (*A*) and statistical data (*B*) on ratio of spleen to body weight are shown for WT and KO mice. (*C*) A comparison showed more erythrocytes in blood isolated from KO than from WT mice and higher levels of hemoglobin in KO serum than in control. (*D–J*) Quantitative analyses were done to determine the number of red blood cells (RBCs), hemoglobin (HGB), hematocrit (HCT), mean corpuscular volume (MCV), mean corpuscular hemoglobin (MCH), red cell distribution width (RCDW), and mean corpuscular hemoglobin concentration (MCHC) values in WT, KO, and KO-R (n = 6). (*K–M*) The numbers of platelet count (PLT), platelet hematocrit (PCT), and platelet distribution width (PDW) were measured in these three groups of mice (n = 6).

Consistent with the animal data, phospho-p38 signals significantly decreased in subjects with a BMI value over 35 (Fig. 7*C*). Thus, there is a reverse correlation between p38 phosphorylation and increase of age or body weight, indicating a progressive inhibition of p38 during development of obesity. In aggregate, our results demonstrate a common signaling pathway, involving p38 inhibition, in adipogenesis and obesity development (Fig. 7*D*).

Discussion

Previously viewed as a depot for storage of excess energy, adipose tissue has been recently recognized as an endocrine gland that secretes adipokines for regulation of multiple physiological processes. However, it is unclear how adipogenesis influences mammalian development and physiology. Results presented here indicate that Shp2 plays a pivotal role in mammalian adipogenesis, as removal of Shp2 inhibits adipocyte differentiation from ES cells in vitro and adipose deletion of Shp2 results in severe lipodystrophy and early postnatal lethality in mice. Partial rescue of mutants' lifespan by fat transplantation argues for an essential role of adipose tissue in mammalian survival and physiology. This important function of Shp2 in adipose physiology was supported by a previous in vitro study, which showed impaired adipogenic differentiation of 3T3-L1 cells by Shp2 knockdown (37). In contrast, Piard et al. reported a clinical case for development of abdominal lipomatosis and subsequently adipose tumor in a Noonan syndrome patient with a heterozygous Gln506Pro mutation in *PTPN11*/*Shp2* (38).

PPARγ is a critical gene acting in adipogenesis, and its expression is coordinately regulated by various cytokines/hormones and signaling pathways. Shp2 promotes the expression of PPARγ to mediate adipogenesis or metabolic functions. By examining multiple signaling components upstream, we demonstrated upregulation of phospho-p38 signal in Shp2-deficient adipocytes, in contrast to suppression of Erk activation, suggesting a mechanism for Shp2 action by inhibiting p38 activity. Overactivated p38 leads to higher phosphorylation and accelerated degradation of histone acetyltransferase p300, a target of p38 kinase. It is interesting to note that a decreased amount of p300 caused selectively impaired expression of PPARγ with no effect on C/EBPβ in Shp2-deficient adipocytes. Previous experiments have shown that TAO family kinases activate MKK3/6 that in turn phosphorylate and activate p38 (13, 33, 34). Results obtained in this study suggest a negative role of Shp2 on p38 activation, likely via a direct effect on TAO2

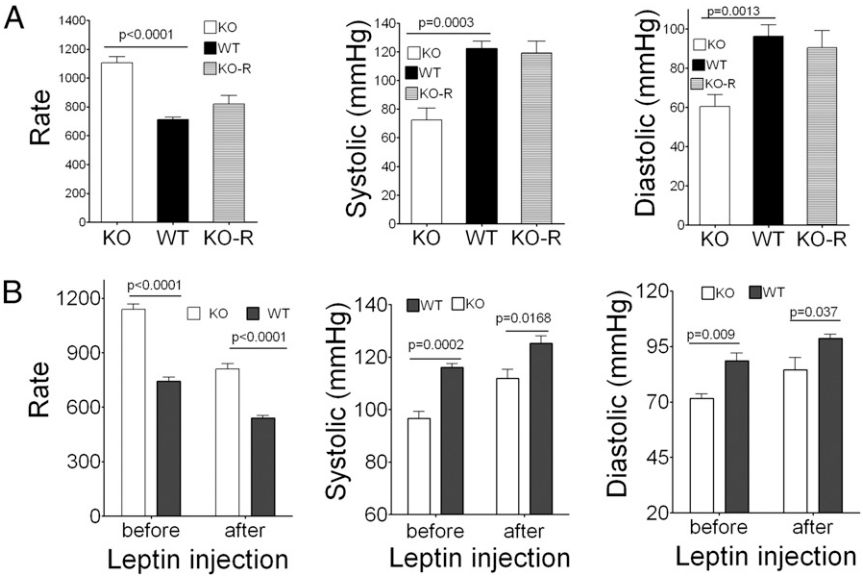

Fig. 5. Fat transplant or leptin injection restores blood pressure in $Shp2^{fat-/-}$ mice. (*A*) The heart beat rate and systolic and diastolic blood pressure were measured for WT (n = 7), KO (n = 7), and KO-R (n = 6) mice. (*B*) The effect of leptin administration on blood pressure was determined in WT and KO mice.

kinase, in adipogenesis, although more detailed analysis is required to elucidate the biochemical mechanism.

The impaired transcription of PPARγ is at least in part responsible for defective adipogenesis and lack of WAT in $Shp2^{fat-/-}$ mice. Consistently, *aP2-Cre*–mediated deletion of PPARγ also causes similar phenotypes of lipodystrophy (23, 39). Of note, the phenotype of adipose-specific PPARγ knockout mice is not as severe as that of $Shp2^{fat-/-}$ mice, suggesting that Shp2 elimination affects other adipogenic pathways in addition to defective PPARγ expression. Inhibition of PPARγ signaling leads to progressive development of lipodystrophy, which is consistent with acquired lipodystrophy in human subjects (40, 41). Accumulating data suggest that Wnt, TGF, Insulin/IGF, EGF, FGF, and other cytokines can regulate adipogenesis through PPARγ signaling (42). Shp2 has been shown to modulate intracellular signaling events elicited by many of these growth factors and other extracellular cues (21, 22). It is conceivable that Shp2 may act to integrate and coordinate multiple upstream signals in promoting adipogenesis and, therefore, deletion of Shp2 leads to a very severe phenotype of lipodystrophy. However, further experiments are required for identification of specific upstream signals that upregulate the catalytic activity of this tyrosine phosphatase and for determination of how activated Shp2 enzyme regulates the p38 pathway in adipocytes.

The essential role of Shp2 in adipogenesis is very similar to its requirement for hematopoiesis (21). In previous work, we have shown that homozygous deletion of Shp2 blocks ES cell differentiation into all blood cell lineages in vitro and in vivo (43–46). However, distinct biochemical mechanisms are likely involved in Shp2 functions in hematopoiesis and adipogenesis. As described above, Shp2 acts to promote PPARγ expression and adipocyte differentiation via suppression of p38, whereas its action in hematopoiesis may involve reciprocal regulation of Erk and Stat3 pathways (21). More recent experimental data suggest an interesting Kit-Shp2-*Kit* signaling circuit in hematopoietic stem/progenitor cells (47).

Several lines of evidence suggest strongly that Shp2-mediated inhibition of p38 is a critical signaling event driving adipocyte differentiation. Phospho-p38 levels were markedly elevated in Shp2 knockout and knockdown preadipocytes and adipocytes. Increased p38 activation leads to accelerated p300 degradation and consequently down-regulation of PPARγ expression. Notably, p38 inhibition restored adipocyte differentiation of $Shp2^{-/-}$ ES cells. We also provide experimental results indicating a similar effect of p38 inhibition in development of obesity in adults. As shown in Fig. 7, p38 phosphorylation progressively decreased during development of obesity and in aging mice. Moreover, phospho-p38 signal strength was inversely correlated with the BMI value in human subjects. Thus, we propose that a signaling mechanism involving p38 suppression is shared by adipogenesis and pathological adipose expansion in obese subjects. Consistently, dramatically decreased p38 kinase activity was detected in fat tissue in *ob*/*ob* mice and HFD-induced obese mice (14). However, there are also reports suggesting an opposite effect of p38 in promoting adipogenesis, as adipocyte differentiation from 3T3-L1 preadipocytes was suppressed by treatment with the p38 inhibitor SB203580 or by expression of a dominant negative mutant of p38 (12). In contrast, overexpression of a constitutively active MKK6 mutant enhances adipogenic activity of 3T3-L1 cells (13). These conflicting data may be due to phosphorylation of different substrates by p38, as influenced by p38 expression levels or cellular context.

$Shp2^{fat-/-}$ mice suffered from lipodystrophy with hypotension and extremely low serum levels of leptin. Fat transplantation and leptin administration partially restored blood pressure, providing the direct evidence that leptin is a critical adipokine that regulates blood pressure. Consistently, human leptin deficiency causes hypotension and increases mortality in childhood after infections (48, 49). Prolonged caloric restriction and reduced leptin levels effectively decrease blood pressure in humans and rodents suffering hypotension (28, 50, 51). In contrast, obese patients are associated with hypertension due to hyperleptinemia (28–30, 51, 52).

Either by genetic inheritance or through drugs or viral infection, patients with lipodystrophy syndrome display multiple metabolic disorders, including insulin resistance, lack of circulating leptin, cardiac hypertrophy, hepatic steatosis, and hypertriglyceridemia (53, 54). Many animal models have been reported for lipodystrophy, with variable or opposite metabolic complications associated with the syndrome (55–61). The adipose-specific PPARγ knockout mouse lines generated by several groups exhibit different phenotypes (23, 39). Of note, the $Shp2^{fat-/-}$ mice present the most severe phenotype of lipodystrophy with early postnatal lethality and low blood pressure. There are several

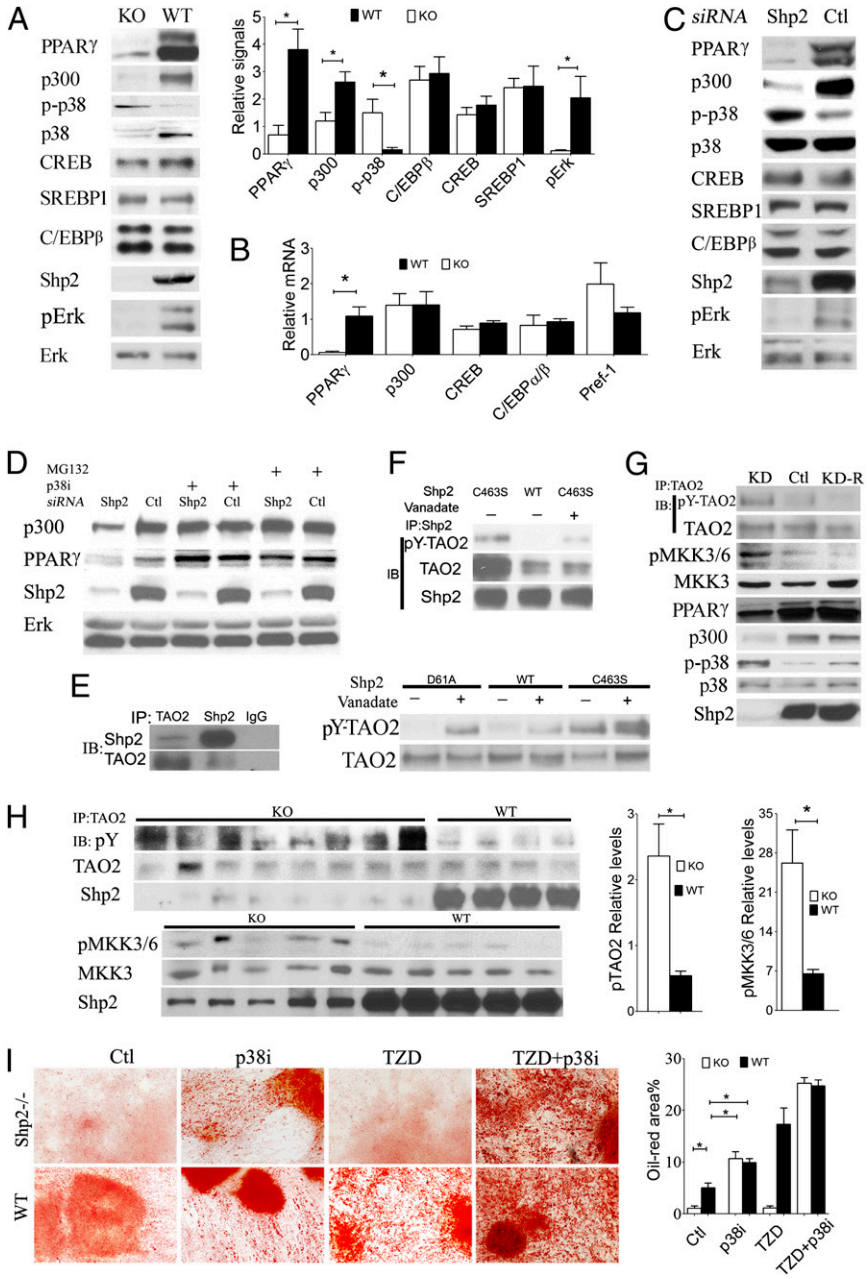

Fig. 6. Shp2 promotes PPARγ expression through inhibition of p38. (*A*) (*Left*) Immunoblot analysis was performed on WT and KO adipose tissue lysates, using antibodies as indicated. (*Right*) Signals were quantified by ImageJ software ($n = 4–8$). (*B*) Real-time Q-PCR was performed to detect mRNA levels in WT and KO adipose as indicated, using β-actin as a control ($n = 4–8$). (*C*) Immunoblotting was performed in control and Shp2 knockdown 3T3-L1 cells, using antibodies as indicated. Similar results were obtained in at least three independent experiments. (*D*) Control and Shp2 knockdown 3T3-L1 cells were treated with proteasome inhibitor MG132 or p38 inhibitor (p38i). Cell lysates were immunoblotted using antibodies as indicated. Similar results were obtained in at least three independent experiments. (*E*) (*Left*) Coimmunoprecipitation between Shp2 and TAO2. (*Right*) PTP assay in vitro between Shp2 and TAO2 with or without vanadate (10 mM). (*F*) Substrate trapping with or without vanadate (10 mM). $Shp2^{WT}$ and $Shp2^{C463S}$ (C/S) were expressed in 3T3-L1 cells. Immunoprecipitation was done with anti-flag antibody and immunoblotted with either anti-pY or anti-TAO2 antibody. Similar results were obtained in at least three independent experiments. (*G*) Shp2 was reintroduced in Shp2 knockdown 3T3-L1 cells (KD-R), and signals of PPARγ, p300, p-p38, pMKK3/6, and pTAO2 were examined. (*H*) Immunoblot analysis was performed on WT and KO adipose tissue lysates, using antibodies against pY, TAO2, pMKK3/6, or MKK3. (*I*) Cultured WT and $Shp2^{-/-}$ ES cells were allowed to differentiate into adipocytes in vitro, with p38 inhibitor SB220025 (10 nM) and/or PPARγ antagonist Rosiglitazone (2 μM) added to culture medium. (*Left*) Representative oil-red staining images. (*Right*) Oil-red staining was quantified by ImageJ software.

other unique features for this animal model, such as lack of WAT with normal BAT, normal insulin signaling, normal serum profiles of lipids, and hepatic steatosis. Further characterization of this mouse model will provide unique insights into the molecular mechanism for adipogenesis and better therapeutic targets for obesity.

Experimental Procedures

Mouse Lines. Generation of the conditional Shp2 mutant allele ($Shp2^{flox}$) was reported previously (18). The *aP2-Cre* transgenic mouse line originally generated in the Evans laboratory (21) was provided by J. Olefsky at University of California at San Diego (UCSD). The *adiponectin-Cre* (23) and *LysM-Cre* mice (27) were purchased from JAX. All strains of mice were at C57BL/6 background. Mice at age 4–8 wk were used to perform experiments and

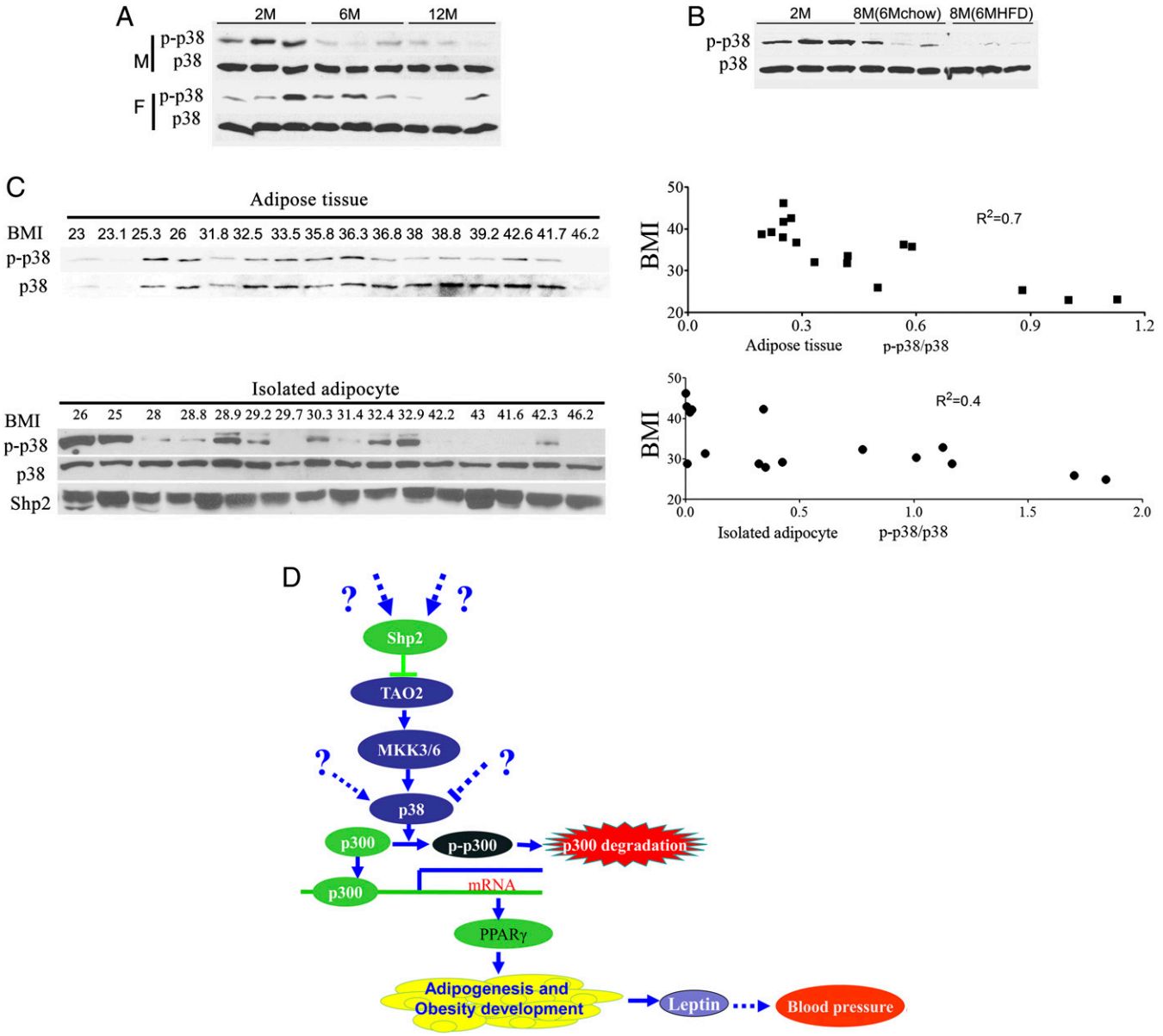

Fig. 7. p-p38 levels decreased in aged or obese animals and obese human subjects. (*A*) Immunoblot analysis was performed to determine p-p38 levels and p38 protein amounts in adipose tissue isolated from male and female mice at age 2, 6, and 12 mo. (*B*) p-p38 levels were evaluated by immunoblot analysis in adipose tissue isolated from mice at age 2 or 8 mo fed regular chow food or from 8-mo old mice that were fed HFD for 6 mo. (*C*) p-p38 and p38 were determined in adipose tissue (*Upper*) and isolated adipocytes (*Lower*) from subjects with different BMI values. (*Right*) The relative p-p38/p38 was plotted against BMI, showing a negative correlation. (*D*) A model for Shp2 promotion of adipogenesis through inhibition of p38 and adipose tissue secretion of leptin to regulate blood pressure.

collect tissues. All animal procedures were approved by the Institutional Animal Care and Use Committees at University of California at San Diego or Sanford/Burnham Medical Research Institute.

Metabolic Assays. Complete blood cell (CBC) counting was performed with the VetScan HMII Hematology System (Abaxis). Serum was collected from mice at age 4–12 wk. Serum insulin and leptin levels were measured using commercial kits (90030 and INSKR020; Crystal Chem). Adipokines were measured by Luminex (Millipore). IGF1 was measured by IGF1 Luminex (Millipore). Total triglyceride was measured by an ELISA kit (Cayman Chemical; 10010303). Cholesterol, HDL, and LDL/VLDL were measured by the colorimetric method (BioAssay Systems). Mice at age 4–8 wk were warmed up to 35 °C on a heating pad to acclimate the measurement of blood pressure for 20 min, and leptin [3 μg/kg body weight (BW); National Hormone and Peptide Program or Calbiochem] was injected intraperitoneally. The CODA-6 system (Kent Scientific) was used to monitor the blood pressure of mice from 9:00 AM to 11:00 AM.

Fat Transplantation. Fat transplantation was performed as previously described (62). In brief, s.c. and gonadal fat pads were collected from WT littermates of the same sex at age at least 1 mo. Fat pads were cut into small pieces (about 2 mm diameter) and kept in saline at 37 °C for transplantation. *Shp2*$^{fat-/-}$ recipients were anesthetized by isoflurane or i.p. injection with avertin. Skin was freed from connective tissue, using blunt dissection, and one piece of fat was inserted into one incision. Each mouse received a total of five to six donor slices of fat pad inserted into the s.c. area, i.e., below the skin on the back. The incisions were sutured, and the mice were allowed to recover from anesthesia before return to their home cages. The sham mice underwent the same surgery but did not receive fat transplant.

Cell Signaling. Cells (3T3-L1) (ATCC) were cultured under standard conditions. Gonadal fat pads from mice at age 4–8 wk were isolated for experiments. Fat tissue lysates were prepared in tissue lysis buffer. Cell or tissue lysates were immunoblotted with antibodies to Shp2, SREBP1, C/EBPβ, p300, CREB, F4/80, TAO2 antibody (Santa Cruz Biotechnology), PPAR$\gamma_{1/2}$, phospho-p38 (p-p38) and

p38, or Erk (Cell Signaling). Shp2-specific siRNA was used to knock down Shp2 expression, using the Amaxa nucleofector method. MG132 (Sigma) was used to inhibit protein degradation, and p38 chemical inhibitors SB203580 (Calbiochem) and SB220025 (Sigma) were used to suppress p38 kinase activity. Shp2-Flag, Shp2D/A, Shp2C/S, TAO1, TAO2, MKK3-Flag, MKK4-Flag, MKK6-Flag, or p38-Flag plasmids were transiently transfected into 293 cells. Purified proteins by anti-Flag beads (M2; Sigma) were used to perform a tyrosine phosphatase assay in vitro. Anti–p-Y antibodies [4G10 (Upstate) and PY99 (Santa Cruz Biotechnology)] were used to detect tyrosine phosphorylation of proteins.

Real-time quantitative (Q)-PCR was performed using total RNA extracted from adipose tissue by the TRIzol method. cDNAs were synthesized by an RT kit (Invitrogen). Primers of PPARγ, 5′-CAAAACACCAGTGTGAATTA-3′, 5′-ACCATGGTAATTTCTTGTGA-3′; p300, 5′-TCTGGGTGCAAAGATGTTCA-3′, 5′-GCAGCTGCCCCTGTATATTA-3′; β-actin, 5′-CTGCGTTTTACACCCTTTCTTTG-3′, 5′-GCCATGCCAATGTTGTCTCTTAT-3′; Pref1, 5′-AGTGCGAAACCTGGGTGTC-3′, 5′-GCCTCCTTGTTGAAAGTGGTCA-3′; C/EBPβ, CAAGAACAGCAACGAGTACCG-3′, 5′-GTCACTGGTCAACTCCAGCAC-3′; CREB, 5′-AGGATCTTCTGCCGTCTTGAT-3′, 5′-GCGCAGCCTTCAGTCTCAT-3′; and FASN, 5′-GGAGGTGGTGATAGCCGGTAT-3′, 5′-TGGGTAATCCATAGAGCCCAG-3′ were used for PCR amplification. Use of human samples was approved by Veteran's Administration Hospital and UCSD committees.

Adipocyte Differentiation from ES Cells. Shp2$^{-/-}$ and WT mouse ES cells were maintained in DMEM with leukemia inhibitory factor and 15% (vol/vol) FBS (36). Adipocyte differentiation was performed as reported previously (63). Briefly, ES cells were allowed to form embryoid bodies and then treated with 0.1 μM *all-trans* retinoic acid (Sigma) from days 2 and 7. From day 13 to the end of the differentiation process, cells were treated with a mixture of 85 nM insulin and 0.5 mM 3-isobutyl-1-methylxanthine (Sigma). Insulin-transferrin-selenium-X (Gibco) was added every day to the culture medium to induce ES cell differentiation. Adipocyte differentiation was evaluated by oil-red staining after 28 d of embryoid body formation.

Statistical Analysis. ImageJ software was used to quantify data. Statistical significance was determined with an unpaired two-tailed Student's *t* test and analysis of variance, and data were expressed as the mean ± SEM.

ACKNOWLEDGMENTS. The authors thank Drs. J. Olefsky for providing *aP2-Cre* mice, H. J. Kung for providing TAO1/2/3 plasmids, and P. Scherer for insightful suggestion and advice. We also thank F. Princen for setting up the animal breeding at the initial stage and our colleagues for helpful discussion and support. This work was supported by National Institutes of Health Grants R01DK073945 and DK075916 (to G.-S.F.).

1. Spiegelman BM, Flier JS (2001) Obesity and the regulation of energy balance. *Cell* 104(4):531–543.
2. Flier JS (2004) Obesity wars: Molecular progress confronts an expanding epidemic. *Cell* 116(2):337–350.
3. Zhang Y, et al. (1994) Positional cloning of the mouse obese gene and its human homologue. *Nature* 372(6505):425–432.
4. Friedman JM, Halaas JL (1998) Leptin and the regulation of body weight in mammals. *Nature* 395(6704):763–770.
5. Rosen ED, Spiegelman BM (2000) Molecular regulation of adipogenesis. *Annu Rev Cell Dev Biol* 16:145–171.
6. Tontonoz P, Hu E, Spiegelman BM (1994) Stimulation of adipogenesis in fibroblasts by PPAR gamma 2, a lipid-activated transcription factor. *Cell* 79(7):1147–1156.
7. Freytag SO, Paielli DL, Gilbert JD (1994) Ectopic expression of the CCAAT/enhancer-binding protein alpha promotes the adipogenic program in a variety of mouse fibroblastic cells. *Genes Dev* 8(14):1654–1663.
8. Tontonoz P, Spiegelman BM (2008) Fat and beyond: The diverse biology of PPARgamma. *Annu Rev Biochem* 77:289–312.
9. Meyer MR, et al. (2012) Deletion of G protein-coupled estrogen receptor increases endothelial vasoconstriction. *Hypertension* 59(2):507–512.
10. Badri KR, Zhou Y, Dhru U, Aramgam S, Schuger L (2008) Effects of the SANT domain of tension-induced/inhibited proteins (TIPs), novel partners of the histone acetyltransferase p300, on p300 activity and TIP-6-induced adipogenesis. *Mol Cell Biol* 28(20):6358–6372.
11. Ohoka N, Kato S, Takahashi Y, Hayashi H, Sato R (2009) The orphan nuclear receptor RORalpha restrains adipocyte differentiation through a reduction of C/EBPbeta activity and perilipin gene expression. *Mol Endocrinol* 23(6):759–771.
12. Engelman JA, Lisanti MP, Scherer PE (1998) Specific inhibitors of p38 mitogen-activated protein kinase block 3T3-L1 adipogenesis. *J Biol Chem* 273(48):32111–32120.
13. Engelman JA, et al. (1999) Constitutively active mitogen-activated protein kinase kinase 6 (MKK6) or salicylate induces spontaneous 3T3-L1 adipogenesis. *J Biol Chem* 274(50):35630–35638.
14. Aouadi M, et al. (2006) Inhibition of p38MAPK increases adipogenesis from embryonic to adult stages. *Diabetes* 55(2):281–289.
15. Li C, Friedman JM (1999) Leptin receptor activation of SH2 domain containing protein tyrosine phosphatase 2 modulates Ob receptor signal transduction. *Proc Natl Acad Sci USA* 96(17):9677–9682.
16. Bjorbak C, et al. (2000) SOCS3 mediates feedback inhibition of the leptin receptor via Tyr985. *J Biol Chem* 275(51):40649–40657.
17. Krajewska M, et al. (2008) Development of diabesity in mice with neuronal deletion of Shp2 tyrosine phosphatase. *Am J Pathol* 172(5):1312–1324.
18. Zhang EE, Chapeau E, Hagihara K, Feng GS (2004) Neuronal Shp2 tyrosine phosphatase controls energy balance and metabolism. *Proc Natl Acad Sci USA* 101(45):16064–16069.
19. Banno R, et al. (2010) PTP1B and SHP2 in POMC neurons reciprocally regulate energy balance in mice. *J Clin Invest* 120(3):720–734.
20. He Z, et al. (2012) Shp2 controls female body weight and energy balance by integrating leptin and estrogen signals. *Mol Cell Biol* 32(10):1867–1878.
21. Chan RJ, Feng GS (2007) PTPN11 is the first identified proto-oncogene that encodes a tyrosine phosphatase. *Blood* 109(3):862–867.
22. Lai LA, Zhao C, Zhang EE, Feng GS (2004) The Shp-2 tyrosine phosphatase. *Protein Phosphatases, Topics in Current Genetics*, eds Arino J, Alexander D (Springer, Berlin), Vol 5, pp 275–299.
23. He W, et al. (2003) Adipose-specific peroxisome proliferator-activated receptor gamma knockout causes insulin resistance in fat and liver but not in muscle. *Proc Natl Acad Sci USA* 100(26):15712–15717.
24. Zabolotny JM, et al. (2008) Protein-tyrosine phosphatase 1B expression is induced by inflammation in vivo. *J Biol Chem* 283(21):14230–14241.
25. Eguchi J, et al. (2011) Transcriptional control of adipose lipid handling by IRF4. *Cell Metab* 13(3):249–259.
26. Bettaieb A, et al. (2011) Adipose-specific deletion of Src homology phosphatase 2 does not significantly alter systemic glucose homeostasis. *Metabolism* 60(8):1193–1201.
27. Clausen BE, Burkhardt C, Reith W, Renkawitz R, Förster I (1999) Conditional gene targeting in macrophages and granulocytes using LysMcre mice. *Transgenic Res* 8(4):265–277.
28. Ashida T, Ono C, Sugiyama T (2007) Effects of short-term hypocaloric diet on sympatho-vagal interaction assessed by spectral analysis of heart rate and blood pressure variability during stress tests in obese hypertensive patients. *Hypertens Res* 30(12):1199–1203.
29. Rahmouni K, et al. (2008) Leptin resistance contributes to obesity and hypertension in mouse models of Bardet-Biedl syndrome. *J Clin Invest* 118(4):1458–1467.
30. Hall JE, et al. (2010) Obesity-induced hypertension: Role of sympathetic nervous system, leptin, and melanocortins. *J Biol Chem* 285(23):17271–17276.
31. Takahashi N, et al. (2002) Overexpression and ribozyme-mediated targeting of transcriptional coactivators CREB-binding protein and p300 revealed their indispensable roles in adipocyte differentiation through the regulation of peroxisome proliferator-activated receptor gamma. *J Biol Chem* 277(19):16906–16912.
32. Poizat C, Puri PL, Bai Y, Kedes L (2005) Phosphorylation-dependent degradation of p300 by doxorubicin-activated p38 mitogen-activated protein kinase in cardiac cells. *Mol Cell Biol* 25(7):2673–2687.
33. Yustein JT, et al. (2003) Comparative studies of a new subfamily of human Ste20-like kinases: Homodimerization, subcellular localization, and selective activation of MKK3 and p38. *Oncogene* 22(40):6129–6141.
34. Takekawa M, Tatebayashi K, Saito H (2005) Conserved docking site is essential for activation of mammalian MAP kinase kinases by specific MAP kinase kinase kinases. *Mol Cell* 18(3):295–306.
35. Urs S, Harrington A, Liaw L, Small D (2006) Selective expression of an aP2/Fatty Acid Binding Protein 4-Cre transgene in non-adipogenic tissues during embryonic development. *Transgenic Res* 15(5):647–653.
36. Wu D, et al. (2009) A conserved mechanism for control of human and mouse embryonic stem cell pluripotency and differentiation by shp2 tyrosine phosphatase. *PLoS ONE* 4(3):e4914.
37. Uehara T, et al. (2007) SHP-2 positively regulates adipogenic differentiation in 3T3-L1 cells. *Int J Mol Med* 19(6):895–900.
38. Piard J, et al. (2012) Extensive abdominal lipomatosis in a patient with Noonan/LEOPARD syndrome (Noonan syndrome-Multiple Lentigines). *Am J Med Genet A* 158A(6):1406–1410.
39. Jones JR, et al. (2005) Deletion of PPARgamma in adipose tissues of mice protects against high fat diet-induced obesity and insulin resistance. *Proc Natl Acad Sci USA* 102(17):6207–6212.
40. Shrivastav S, et al. (2008) Human immunodeficiency virus (HIV)-1 viral protein R suppresses transcriptional activity of peroxisome proliferator-activated receptor gamma and inhibits adipocyte differentiation: Implications for HIV-associated lipodystrophy. *Mol Endocrinol* 22(2):234–247.
41. Caron M, Vigouroux C, Bastard JP, Capeau J (2009) Antiretroviral-related adipocyte dysfunction and lipodystrophy in HIV-infected patients: Alteration of the PPARγ-dependent pathways. *PPAR Res* 2009:507141.
42. Cristancho AG, Lazar MA (2011) Forming functional fat: A growing understanding of adipocyte differentiation. *Nat Rev Mol Cell Biol* 12(11):722–734.
43. Qu CK, et al. (1997) A deletion mutation in the SH2-N domain of Shp-2 severely suppresses hematopoietic cell development. *Mol Cell Biol* 17(9):5499–5507.
44. Qu CK, et al. (1998) Biased suppression of hematopoiesis and multiple developmental defects in chimeric mice containing Shp-2 mutant cells. *Mol Cell Biol* 18(10):6075–6082.
45. Qu CK, Nguyen S, Chen J, Feng GS (2001) Requirement of Shp-2 tyrosine phosphatase in lymphoid and hematopoietic cell development. *Blood* 97(4):911–914.
46. Chan RJ, Johnson SA, Li Y, Yoder MC, Feng GS (2003) A definitive role of Shp-2 tyrosine phosphatase in mediating embryonic stem cell differentiation and hematopoiesis. *Blood* 102(6):2074–2080.

47. Zhu HH, et al. (2011) Kit-Shp2-Kit signaling acts to maintain a functional hematopoietic stem and progenitor cell pool. *Blood* 117(20):5350–5361.
48. Ozata M, Ozdemir IC, Licinio J (1999) Human leptin deficiency caused by a missense mutation: Multiple endocrine defects, decreased sympathetic tone, and immune system dysfunction indicate new targets for leptin action, greater central than peripheral resistance to the effects of leptin, and spontaneous correction of leptin-mediated defects. *J Clin Endocrinol Metab* 84(10):3686–3695.
49. Fischer-Posovszky P, et al. (2010) A new missense mutation in the leptin gene causes mild obesity and hypogonadism without affecting T cell responsiveness. *J Clin Endocrinol Metab* 95(6):2836–2840.
50. de Luis DA, Aller R, Izaola O, Sagrado MG, Conde R (2008) Modulation of adipocytokines response and weight loss secondary to a hypocaloric diet in obese patients by -55CT polymorphism of UCP3 gene. *Horm Metab Res* 40(3):214–218.
51. Swoap SJ (2001) Altered leptin signaling is sufficient, but not required, for hypotension associated with caloric restriction. *Am J Physiol Heart Circ Physiol* 281(6):H2473–H2479.
52. Konukoglu D, Serin O, Turhan MS (2006) Plasma leptin and its relationship with lipid peroxidation and nitric oxide in obese female patients with or without hypertension. *Arch Med Res* 37(5):602–606.
53. Garg A (2004) Acquired and inherited lipodystrophies. *N Engl J Med* 350(12):1220–1234.
54. Joffe BI, Panz VR, Raal FJ (2001) From lipodystrophy syndromes to diabetes mellitus. *Lancet* 357(9266):1379–1381.
55. Cortés VA, et al. (2009) Molecular mechanisms of hepatic steatosis and insulin resistance in the AGPAT2-deficient mouse model of congenital generalized lipodystrophy. *Cell Metab* 9(2):165–176.
56. Duan SZ, et al. (2007) Hypotension, lipodystrophy, and insulin resistance in generalized PPARgamma-deficient mice rescued from embryonic lethality. *J Clin Invest* 117(3): 812–822.
57. El-Haschimi K, et al. (2003) Insulin resistance and lipodystrophy in mice lacking ribosomal S6 kinase 2. *Diabetes* 52(6):1340–1346.
58. Olswang Y, et al. (2002) A mutation in the peroxisome proliferator-activated receptor gamma-binding site in the gene for the cytosolic form of phosphoenolpyruvate carboxykinase reduces adipose tissue size and fat content in mice. *Proc Natl Acad Sci USA* 99(2):625–630.
59. Pajvani UB, et al. (2005) Fat apoptosis through targeted activation of caspase 8: A new mouse model of inducible and reversible lipoatrophy. *Nat Med* 11(7):797–803.
60. Moitra J, et al. (1998) Life without white fat: A transgenic mouse. *Genes Dev* 12(20): 3168–3181.
61. Gavrilova O, et al. (2000) Surgical implantation of adipose tissue reverses diabetes in lipoatrophic mice. *J Clin Invest* 105(3):271–278.
62. Tran TT, Yamamoto Y, Gesta S, Kahn CR (2008) Beneficial effects of subcutaneous fat transplantation on metabolism. *Cell Metab* 7(5):410–420.
63. Aouadi M, et al. (2006) p38 mitogen-activated protein kinase activity commits embryonic stem cells to either neurogenesis or cardiomyogenesis. *Stem Cells* 24(5): 1399–1406.
64. Bottini N, Bottini E, Gloria-Bottini F, Mustelin T (2002) Low-molecular-weight protein tyrosine phosphatase and human disease: In search of biochemical mechanisms. *Arch Immunol Ther Exp* 50(2):95–104.